*Mausam*, (1997), 48, 1, 1-8

551.509.327 : 551.508.826

# Prediction of satellite track of tropical cyclone from spiral bands

BRIJ BHUSHAN

*Meteorological Office, New Delhi*

*(Received 9 April 1992, Modified 15 July 1996)*

**सार** — जब चक्रवात की तीव्रता टी-5.0 होती है तब उसके केन्द्र के आस-पास के बादलों के घेरे को जिस क्षेत्र में बादलों की सर्पिल पट्टी छूती है वह क्षेत्र बदलता रहता है । इसे चक्रवात के उपग्रह से प्राप्त पराबैगनी उभारे हुए चित्रों में सुगमता से पहचाना जा सकता है । यह बताया गया है कि चक्रवात के केन्द्र से उठने वाले तथा बादलों के घेरे के इस विशेष क्षेत्र से गुजरने वाले वेक्टर से उष्णकटिबंधीय चक्रवात के आगामी उपग्रह-पथ का पता चलता है । अपने जीवन काल के एक समय में पहचान की ऊपर बताई गई विशेषताएँ रखने वाले दो चक्रवातों के आँकड़े प्रेक्षणात्मक त्रुटियों की सीमा के भीतर इस तर्कसंगत तथ्य के अनुरूप पाए गए हैं ।

**ABSTRACT.** The sector of the eye wall where a spiraling convective band appears to fasten with it changes and oscillates over the eye wall and such a sector is easily discernible in Enhanced Infra Red (EIR) imagery received from satellite for a cyclone whose intensity is more than T5.0. It has been argued that a vector having initial point at the centre of the cyclone and passing through this particular sector of the eye wall, indicates the future satellite track of a tropical cyclone. The data of the two cyclones, which were showing above mentioned identifiable feature during a part of their lives, withstood the logic within observational errors.

**Key words** — Tropical cyclone, Spiral band, Joining Sector (JS), Enhanced Infra Red (EIR), Direction of movement.

## 1. Introduction

Spiral bands of a tropical cyclone seen in a satellite imagery have been used by Dvorak (1984) for estimating the strength of the tropical cyclone. Fett and Brand (1975) noted that changes in the location of major structural features of the storm are correlated with changes in the direction of movement of the storm centre. One of the features noted was that clear areas or relatively clear areas are often noted as slots in the space between the edge of the central overcast disc and impinging convective bands. These slots apparently rotate as the storm changes direction. Taking these slots as pointers to the new successive position of cyclone they constructed forecast tracks. Another similar feature of the storm in a different form has been exploited here to estimate the direction of motion of a storm and a viable logic has been proposed to justify the approach given here. This is the aim of the present study.

There are a number of studies proposing possible physical mechanisms to explain the formation of spiral bands. Accounts of such studies are given by Anthes (1982). Mention of some of these as are of direct relevance to us will be worthwhile. Senn *et al.* (1957) defined spiral bands with the equation $ln\,(r - r_0) = A + B\,\lambda$, where $r$ is radius, $\lambda$ is azimuth, $r_0$ is the radius of a limiting circle with centre coincident with the storm centre, and is a constant that measures the angular origin of the spiraling band. Here, we shall be interested in angular origin of a spiral band from the wall cloud. Senn and Hiser (1959) noted that the bands formed near the eye and propagate radially outward. They also noted that the bands did not rotate about the storm centre, but instead remain in the quadrant in which they formed. Because of the apparent origin of the bands at the eye wall, they surmised a source of energy which is probably released as it oscillates around the wall cloud. Tatehira (1961) also

showed that bands were generated near the eye and moved outward. On the other hand, Fett and Brand (1975) have noted that major outer rain bands persist for long periods of time in the same location relative to the storm centre. Anthes (1982) is of the opinion that it is likely that these large scale, nearly stationary bands are formed by a different mechanism than the small scale, propagating bands. Faller (1961) proposed that spiral bands were roll vortices which formed from an instability in the boundary layer and took a spiral shape.

Present author also noted that the sector of the eye wall, where a spiral band appears to fasten with eye wall, does change and oscillate over the eye wall. Such a sector can be utilized for estimating the current direction of movement of a tropical cyclone that has developed eye wall and distinct spiral bands. This particular sector of the eye wall at which the spiral cloud band appears to fasten or join with eye wall will be abbreviated as JS (Joining sector) in rest of the text. JS is that part of the periphery of the eyewall where a cloud band joins the eyewall. Thus JS lies in the common area shared by eyewall and impinging band. Angular width of this particular part of the periphery of the eyewall is approximately one fourth of a quadrant.

## 2. Methodology

It can be assumed that the angular origin of the spiral convective band from the eyewall is indicative of the concentration of positive vorticity in that JS of the eyewall as compared to other sectors. The reason to believe so is that larger vertical velocities were found in these parts of spiral bands in a model hurricane (Diercks and Anthes, 1976 a) at the boundary layer. By Ekman layer theory, these vertical velocities, $\omega_h$ are related to geostrophic vorticity, $\xi_g$, in the boundary layer by $\omega_h = \xi_g \left(\frac{k}{2f}\right)^{\frac{1}{2}}$, where $k$ is the eddy viscosity coefficient. Larger are the vertical velocities $\omega_h$, as found in the portion of the spiral band near the eyewall, the larger will be the concentration of positive vorticity in the boundary layer in which such sectors of the eyewall are embedded. Two prominent spiral bands are normally seen clinging to the eyewall at diametrically opposite sectors. It is this symmetry and also closeness of JS's with eye wall, which has been used to identify two JS's out of all other sectors. Such a depiction of a tropical cyclone structure is, of course,

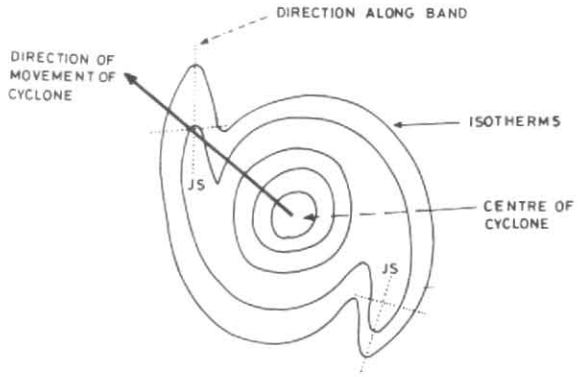


**Fig. 1.** Schematic view of Joining Sectors (JSs) in a tropical cyclone

oversimplified. Movement of the cyclone over past few hours is helpful in deciding as to which of the two JS's has been heading to new positions. It is also noticed that both the JS's are not equally distinct. Identification of JS is ambiguous in a cyclone when its intensity is weaker than T5.0 or so. By distinctness of a JS in Enhanced Infra Red (EIR) imagery we mean the following.

JS is identified in EIR by noting that temperature contours which are more of circular appearance in the eyewall loose this circular nature near JS and take elongated shape. A schematic view is shown in Fig. 1 and a real appearance of JS in EIR imagery can be seen in Figs 2a&b. In Fig. 2a the cyclone is heading towards north and in Fig. 2b it is heading towards northwest. A JS has been taken to be more distinct than the other by its comparatively smooth temperature gradients in the direction of the spiral band as well as transversally. By 'comparative smooth temperature gradients' it was meant that one of the two JS's was having regular isotherms all having nearly the same shape and lay almost parallel to each other. While in other JS the isotherms lack in such characteristics. Temperature gradients along the band and in transversal direction are of the order of 8°C/100 km and 20°C/100 km respectively.

A trough of low temperature in JS is also indicative of stronger secondary circulations in this region and hence larger positive vorticity. It has been seen (Bhushan 1990) that a cyclone moves in the direction of ascendent gradient of positive vorticity tendency, $\vec{\nabla}(\partial\eta/\partial t)$ where $\eta$ is the absolute vorticity. If we further assume that JS is not only the region of higher positive vorticity

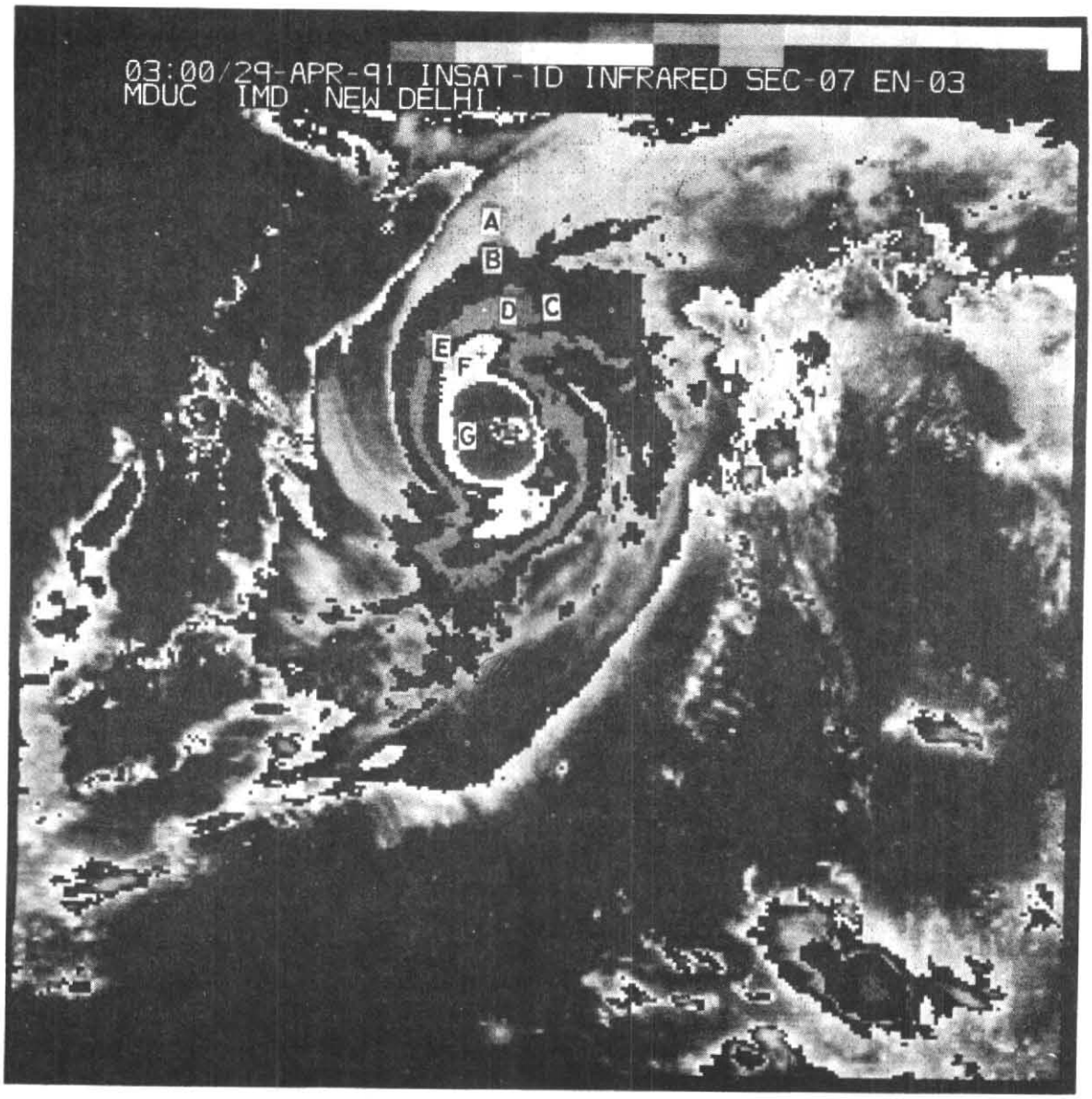


**Fig. 2a.** EIR imagery transmitted by INSAT-ID at 0300 UTC on 29 April 1991. Arrow shows the estimated direction of movement of cyclone. Different gray shades correspond to temperature ranges as; A: 9°C to –30°C, B: –31°C to –41°C, C: –42°C to –53°C, D: –54°C to –63°C, E: –64°C to –69°C, F: –70°C to –75°C, G: –76°C to –80°C and H: < –81°C

but also a place where rate of production of positive vorticity is higher, we can conclude that cyclone's current movement vector can be drawn from cyclone centre to JS. This assumption is seen indirectly to be true for the observations shown in this study.

### 3. Data and analysis

In the Bay of Bengal and the Arabian Sea some of the cyclones attain intensity of T 5.0. (maximum wind of 90 kt) or more and develop spiral bands which can be used to identify JS. Weaker cyclones than T5.0 do not have such clear spiral bands and wall cloud that can allow identification of JS. To find the justification of the above surmised approach for estimating the direction of movement of a tropical cyclone, the directions of movement at different hours of the two cyclones that existed in the Bay of Bengal during 4-9 May 1990 and 23-29 April 1991 and had clear JS (intensity above T5.0) at least during a part of their existence, were determined by the approach illustrated here, *i.e.*, JS's in each of the EIR imageries were identified and the directions of the vectors having

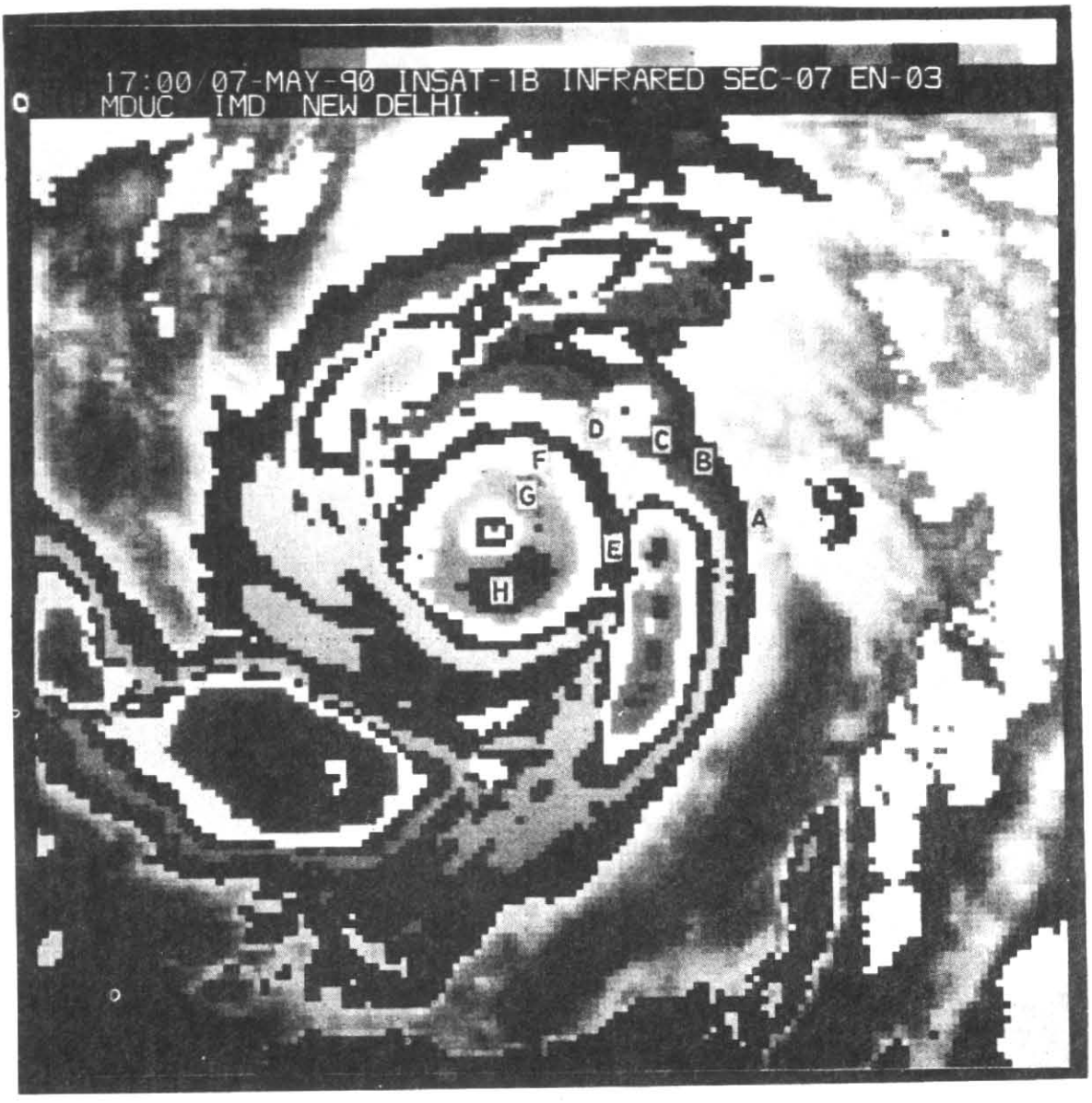


**Fig. 2b.** EIR imagery transmitted by INSAT-IB at 1700 UTC on 7 May 1990. Arrow shows the estimated direction of movement of cyclone. Different gray shades correspond to temperature ranges as; A: 9°C to –30°C, B: –31°C to –41°C, C: –42°C to –53°C, D: –54°C to –63°C, E: –64°C to –69°C, F: –70°C to –75°C, G: –76°C to –80°C and H: < –81°C

origin at the centre of the cyclone and passing through respective JS were noted in sixteen points of compass. In this study, the direction in which both the JS's and the centre of cyclone aligned was taken as the direction of movement of the centre. In several cases while drawing this direction it so happened that line was near the one end of the JS instead of being through the middle of it. This was allowed because accuracy involved here, due to the angular width of JS, is not better than a quarter of a quadrant. These angles, $\theta_t$, (angle $\theta$ at hour '$t$' of the EIR) represented the cyclone's current direction of movement at respective hour/position as seen on satellite pictures. Direction $\phi_t$ (angle $\phi$ at hour '$t$' of the satellite imagery) of movement were also estimated from the lat/long co-ordinates of the cyclone/vortex centre noted operationally at MDUC of IMD, New Delhi for different hours/positions. Values of $\phi_t$ and $\theta_t$ are given in

**TABLE 1**

| Date and hour of observation (UTC) | Position of cyclone in satellite imagery & intensity | | T.No. | Direction of movement of the centre of the cyclone for reaching next position | | Direction of movement as estimated by the location of JS | |
|---|---|---|---|---|---|---|---|
| t | Lat. °N | Long. °E | | $\phi_t$ | $\bar{\phi}_t$ | $\theta_t$ | $\bar{\theta}_t$ |
| **7 May 1990** | | | | | | | |
| 10 | 11.4 | 81.7 | 6.0 | Stationary | — | N | — |
| 11 | 11.4 | 81.7 | | Do | N | NNW | NNW |
| 12 | 11.4 | 81.7 | | N | Do. | NW | Do. |
| 13 | 11.4 | 81.7 | | Stationary | Do. | NNW | Do. |
| 14 | 11.5 | 81.7 | | NNE | NNW | Do. | Do. |
| 15 | 11.7 | 81.8 | | W | Do. | Do. | Do. |
| 16 | 11.7 | 81.6 | | NNW | Do. | Do. | Do. |
| 17 | 11.8 | 81.3 | | NNE | Do. | NW | NW |
| 18 | 12.1 | 81.4 | | NW | N | Do. | Do. |
| 19 | 12.3 | 81.2 | | N | Do. | Do. | Do. |
| 20 | 12.5 | 81.2 | | NE | NNE | Do. | NNW |
| 21 | 12.8 | 81.4 | 6.5 | Do. | Do. | NE | NNE |
| 22 | 12.9 | 81.8 | | N | Do. | Do. | NE |
| 23 | 13.1 | 81.8 | | Do. | N | Do. | Do. |
| **8 May 1990** | | | | | | | |
| 00 | 13.3 | 81.8 | | Stationary | Do. | NNE | NNE |
| 01 | 13.3 | 81.8 | | N | Do. | Do. | Do. |
| 02 | 13.5 | 81.8 | | W | NW | Do. | N |
| 03 | 13.5 | 81.7 | | NW | WNW | NNW | Do. |
| 04 | 13.6 | 81.6 | | WNW | NW | NNE | N |
| 06 | 13.6 | 81.4 | | NW | Do. | Do. | NNE |
| 07* | — | — | | Do. | Do. | Do. | N |
| 08 | 13.7 | 81.3 | | NNW | Do. | NW | Do. |
| 09 | 13.9 | 81.2 | | W | Do. | NNE | Do. |
| 10 | 13.9 | 81.0 | | Stationary | NNW | N | Do. |
| 11 | 13.9 | 81.0 | | NE | NNE | Do. | NNW |
| 12 | 13.9 | 81.1 | | N | Do | NW | Do. |
| 13 | 14.0 | 81.1 | | Do. | N | Do. | Do. |
| 14 | 14.2 | 81.1 | | Do. | Do. | N | Do. |
| 15 | 14.2 | 81.0 | | NNW | — | Do. | — |
| **28 April 1991** | | | | | | | |
| 00 | 15.0 | 87.4 | 5.5 | N | — | N | — |
| 01 | 15.2 | 87.4 | | NNE | NNE | NNE | N |
| 02 | 15.4 | 87.5 | | Do. | Do. | N | Do. |

**TABLE 1 (Contd.)**

| Date and hour of observation (UTC) | Position of cyclone in satellite imagery & intensity | | T No. | Direction of movement of the centre of the cyclone for reaching next position | | Direction of movement as estimated by the location of JS | |
|---|---|---|---|---|---|---|---|
| t | Lat. °N | Long. °E | | $\phi_t$ | $\bar{\phi}_t$ | $\theta_t$ | $\bar{\theta}_t$ |
| **28 April 1991** | | | | | | | |
| 03 | 15.8 | 87.6 | | NE | NE | N | N |
| 04 | 15.9 | 87.7 | | Do. | Do. | Do. | Do. |
| 05 | 16.0 | 87.8 | | N | NNE | NNE | NNE |
| 06 | 16.2 | 87.8 | | Stationary | N | Do. | Do. |
| 07 | 16.2 | 87.8 | | NNE | NNE | N | Do. |
| 08 | 16.4 | 87.9 | | NE | Do. | NNE | N |
| 09 | 16.5 | 88.1 | | N | N | N | NNE |
| 10 | 16.6 | 88.1 | | NW | NNW | NNE | Do. |
| 11 | 16.7 | 88.0 | | Stationary | NNE | Do. | Do. |
| 12 | 16.7 | 88.0 | | E | ENE | NE | NE |
| 13 | 16.7 | 88.2 | | NE | ENE | Do. | Do. |
| 14* | — | — | | Do. | NE | Do. | Do. |
| 15 | 17.0 | 88.6 | | NNE | Do. | Do. | Do. |
| 16 | 17.4 | 88.8 | | NE | NNE | Do. | Do. |
| 17 | 17.5 | 88.9 | | N | Do. | Do. | Do. |
| 18 | 17.8 | 88.9 | 6.0 | NNE | Do. | Do. | Do. |
| 19 | 18.0 | 89.0 | | Do. | Do. | Do. | Do. |
| 20 | 18.2 | 89.0 | | N | N | Do. | Do. |
| 21 | 18.3 | 89.0 | | Do. | Do. | Do. | Do |
| 22 | 18.4 | 89.0 | | Stationary | NNE | NNE | NNE |
| 23 | 18.4 | 89.0 | | NE | Do. | Do. | Do. |
| **29 April 1991** | | | | | | | |
| 00 | 18.5 | 89.1 | 6.5 | NNE | Do. | Do. | Do. |
| 01 | 18.8 | 89.2 | | N | Do. | Do. | Do. |
| 02 | 19.1 | 89.2 | | NE | Do. | N | N |
| 03 | 19.4 | 89.4 | | NNE | Do. | Do. | Do. |
| 04 | 19.6 | 89.5 | | N | N | Do. | Do. |
| 05 | 19.7 | 89.5 | | Do. | NNE | Do. | Do. |
| 06 | 19.8 | 89.5 | 6.0 | NE | Do. | Do. | Do. |
| 07 | 20.0 | 89.7 | | NNE | NE | Do. | Do. |
| 08 | 20.2 | 89.8 | | NE | Do. | Do. | Do. |
| 09 | 20.3 | 89.9 | | Do. | Do. | Do. | Do. |
| 10 | 20.3 | 90.0 | | Do. | Do. | NNE | NNE |
| 11 | 20.5 | 90.3 | | Do. | — | Do. | — |

*Direction of movement interpolated as observations were not available

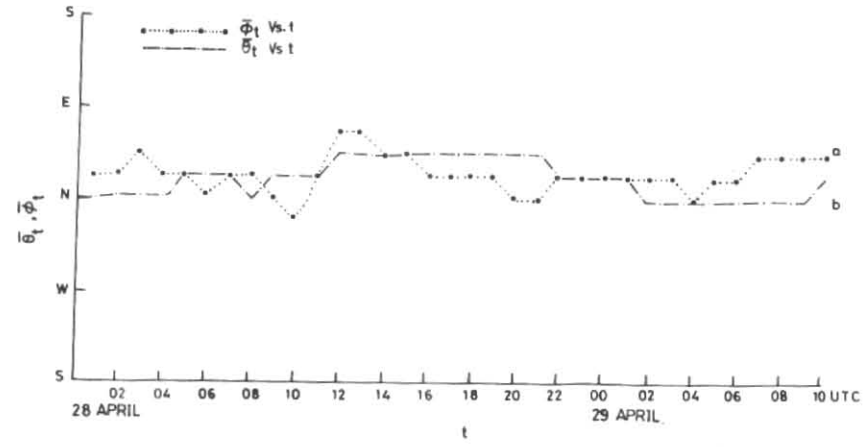


**Fig. 3.** Curve 'a' is a plot of $\bar{\phi}_t$ *vs* $t$ and curve 'b' is a plot of $\bar{\theta}_t$ *vs* $t$ for April 1991 cyclone

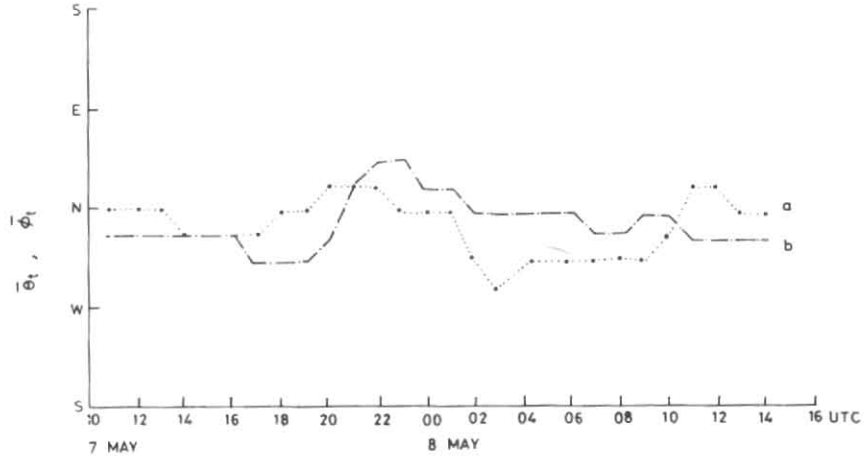


**Fig. 4.** Curve 'a' is a plot of $\bar{\phi}_t$ *vs* $t$ and curve 'b' is a plot of $\bar{\theta}_t$ *vs* $t$ for May 1990 cyclone

Table 1. Data of only those hours have been included for which EIR imageries were available. For missing data the directions have been interpolated for drawing continuous curves in Figs. 3 & 4.

There are limitations on the accuracy with which a centre can be measured on a satellite imagery. In the data set used here the hourly positions of the centre were reported within 0.1 degree of long/lat. The movement of a tropical cyclone over an hour is also of this order. Such data may give direction of hourly motion far from real direction a cyclone centre might have traced. For slow moving cyclone the deviations are still large. It can be seen that such inaccuracies can cause deviations of the order of one quadrant. To reduce errors in the location of the centre of a cyclone, 3-hourly running averages, $\bar{\phi}_t$ of $\phi_t$ were determined. Since the JS has certain extent over eye wall and is not sharper than to give its location in sixteen points of compass, the $\theta_t$ values were also subjected to 3-hourly running averaging. The 3-hourly running means $\bar{\theta}_t$ and $\bar{\phi}_t$ are given in Table. For determining $\bar{\theta}_t$ and $\bar{\phi}_t$ uniform speed was assumed for all $\theta_t$ and $\phi_t$.

Using 3-hourly running means, $(t, \bar{\phi}_t)$ and $(t, \bar{\theta}_t)$ curves were drawn and shown in Fig. 3 as 'a' and 'b' respectively for April 1991 cyclone. Similar curves are given in Fig. 4 for May 1990 cyclone. Comparison of curves 'a' and 'b' in Fig. 3 shows that most of the values of curve 'a' are matching with corresponding values of curves 'b' within one fourth of a quadrant. There are very few points on the two curves which differ by one half of a quadrant.

From the curves 'a' and 'b' of Fig. 4 for May 1990 cyclone we find that only half the points are within one fourth of a quadrant. Except for the point, 03 UTC/8 May 1990, rest half of the points are within error of one half of a quadrant.

The limited set of data used here motivate to accept that JS discerned in EIR can be used for predicting satellite track of a tropical cyclone with an accuracy of one fourth of a quadrant at best. Thus, the logic given above and the data set utilised here broadly support each other. One to one correspondence between $\theta_t$ and $\phi_t$ was masked for many a points perhaps mainly due to the reasons that necessitated their averaging. For taking 3-hourly running means, 'stationary' value of $\phi_t$ was neglected and mean of two instead of three values was taken.

## 4. Conclusion

The procedure built on the logic given in this study for estimating the satellite track of a tropical cyclone can only be useful in those situations where a cyclone has developed such distinct spiral bands as to discern JS. The logic given above for determining the direction of movement although supported by the data set available here, within limits imposed by the data accuracy, yet it requires to be tested over the best fit tracks of the system and a larger data set.

*Acknowledgement*

Author is grateful to DDGM (Sat. Met.), IMD, New Delhi for the encouragement to undertake this study. He is also thankful to Shri D.R. Sikka (Retd. Director, IITM, Pune) for very useful discussions and suggestions.

### References

Anthes, R.A., 1982, "Tropical cyclones their evolution, structure and effects", Meteorological monographs, American Meteorological Society, Vol. **19**, No 41.

Bhushan, B., 1990, "A quantitative approach for determining the movement of depression/cyclone", *Mausam*, **41**, 1, 119-124.

Diercks, J.W. and Anthes, R.A., 1967 a, "Diagnostic studies of spiral rain bands in a non-linear hurricane model", *J. Atmos. Sci.*, **33**, 959-975.

Diercks, J.W. and Anthes, R.A., 1976 b, "A study of spiral bands in a linear model of a cyclonic vortex", *J. Atmos. Sci.*, **33**, 1714-1729.

Dvorak, V.F., 1984, "Tropical cyclone intensity analysis using satellite data", NOAA Tech. Rep., NESDIS, 11.

Faller, A.J., 1961, "An experimental analogy to and proposed explanation of hurricane spiral bands", Second Tech. Conf. Hurrican, Miami, Amer. Meteor. Soc., 307-313.

Fett, R.W. and Brand S., 1975. "Tropical cyclone movement forecasts based on observations from satellites", *J. Appl. Meteor.*, **14**, 452-465.

Senn, H.V., Hiser, H.W. and Bourret, R.C., 1957, "Studies of hurricane spiral bands as observed on radar", Nat. Hur. Res. Proj. Rep. No. 12, 13 p.

Senn, H.V. and Hiser, H.W. 1959, "On the origin of hurricane spiral rain bands", *J. Meteor.*, **16**, 419-426.

Tatehira R., 1961, "A meso-synoptic and radar analysis of typhoon rain band, case study of typhoon "Helen", 1958", Proc. Second Tech. Conf. Hurricanes, Miami, Amer. Meteor. Soc, 115-126.

Weatherford, C.L., 1989, "The structural evolution of typhoons", Colorado State University, Paper No. 446, 198 p.